Highly Robust but Surface-Active: N-Heterocyclic Carbene-Stabilized Au_{25} Nanocluster as a Homogeneous Catalyst

Hui Shen,[§,1] Guocheng Deng,[§,1] Sami Kaappa,[2] Tongde Tan,[1] Yinzi Han,[1] Sami Malola,[2] Shuichao Lin,[1] Boon K. Teo,[1] Hannu Häkkinen,[*,2] Nanfeng Zheng[*,1]

[1]State Key Laboratory for Physical Chemistry of Solid Surfaces, Collaborative Innovation Center of Chemistry for Energy Materials, and National & Local Joint Engineering Research Center for Preparation Technology of Nanomaterials, College of Chemistry and Chemical Engineering, Xiamen University, Xiamen 361005, China.

[2]Departments of Physics and Chemistry, Nanoscience Center, University of Jyväskylä, FI-40014 Jyväskylä, Finland.

KEYWORD. N-heterocyclic carbene, nanocluster, gold, homogeneous catalyst, cycloisomerization.

ABSTRACT: Surface organic ligands play a critical role in stabilizing atomically precise metal nanoclusters in solutions. However, it is still challenging to prepare highly robust ligated metal nanoclusters that are surface-active for liquid-phase catalysis without any pre-treatment. Herein, we report a novel N-heterocyclic carbine-stabilized Au_{25} nanocluster with high thermal and air stabilities as a homogenous catalyst for cycloisomerization of alkynyl amines to indoles. The nanocluster, characterized as $[Au_{25}(^{i}Pr_2\text{-bimy})_{10}Br_7]^{2+}$ ($^{i}Pr_2$-bimy=diisopropyl-benzilidazolium) (**1**), was synthesized by direct reduction of $AuSMe_2Cl$ and $^{i}Pr_2$-bimyAuBr with $NaBH_4$ in one pot. X-ray crystallization analysis revealed that the cluster comprises two centered Au_{13} icosahedra sharing a vertex. Cluster **1** is highly stable and can survive in solution at 80 °C for 12 h, which is superior to Au_{25} nanoclusters passivated with phosphines or thiols. DFT computations reveal the origins of both electronic and thermal stability of **1** and point to the probable catalytic sites. This work provides new insights into the bonding capability of N-heterocyclic carbene to gold in a cluster, and offers an opportunity to probe the catalytic mechanism at the atomic level.

INTRODUCTION

Atomically precise metal nanoclusters (NCs) are expected to combine the advantages of homogeneous and heterogeneous catalysis, and provide an ideal model system for investigating the complicated surface chemistry of metal nanocatalysts.[1-3] For this purpose, the structurally well-defined NCs should be soluble and stable enough in reaction media while having open surface metal sites accessible by reactants.[4-7] To stabilize metal nanoclusters in solutions, one of the most common strategies is to passivate their surface with organic ligands.[8-17] The most common ligands used thus far include phosphines,[18-20] thiols,[21-22] and alkynyls,[23-25] already leading to the successful synthesis and structure solution of a large number of ligated atomically precise metal NCs. While the aforementioned organic ligands are essential in NCs preparation, they often restrict the accessibility of reactants to the catalytic site on the metal cluster surface and, as such, may degrade, or in some cases eliminate the catalytic activity of metal NCs.[26-28] Therefore, limited success has been achieved to demonstrate the direct use of the ligated atomically precise metal NCs as a truly homogeneous catalyst in liquid-phase reactions without being loaded on supports.[4-5, 29]

Recently, N-heterocyclic carbenes (NHCs) have been shown excellent attributes in stabilizing surfaces, nanoparticles or clusters of coinage metals.[30] Several groups have demonstrated that NHCs readily form robust self-assembled monolayer on coinage metal surface and function as a performance-enhancing modifier.[31-36] NHCs stabilized Au nanoparticles with excellent water-solubility, thermal stability, and chemical resistance to thiol exchange have also been reported.[37-38] Several coinage metal clusters stabilized by NHCs have been prepared as well.[39-41] Theoretical work also suggested that NHCs may function as new ligands for gold surface modification and NCs protection.[42] Given these reports, it occurs to us that NHCs may mimic tertiary phosphines as a new class of ligands in stabilizing metal clusters, and may be a game-changer in metal cluster chemistry.[43]

Herein, we report the synthesis, structure, optical property, stability investigation, and catalytic performance of a NHCs stabilized Au_{25} nanocluster, $[Au_{25}(^{i}Pr_2\text{-bimy})_{10}Br_7]^{2+}$(**1**), where ^{i}Pr-bimy is diisopropyl-benzilidazolium. Cluster **1** shows ultra-high thermal and air stability in solution, far better than that of thiolated Au_{25} clusters. More impressively, the cluster also exhibits high catalytic activities as modeled by cycloisomerization of alkynyl amine to indoles. DFT analysis gives a clear view of the electronic structure and optical absorption characteristics of **1**, and points to the probable catalytic sites.

RESULTS AND DISCUSSION

Synthesis and atomic structure. In a typical synthesis of cluster **1**, 0.05 mmol (14.8 mg) $AuSMe_2Cl$ was first dissolved in ethanol, and after ultrasonication, equimolar $^{i}Pr_2$-bimyAuBr was added. After stirring for 15 min, freshly-prepared $NaBH_4$ in ethanol was added dropwise. The suspension gradually dissolved and the solution turns from pale brown to finally dark brown in 2 min. The reaction continued for 20 h at 20 °C in the

dark. After that, excess $NaNO_3$ was added to the reaction mixture. After stirring for 30 min, it was centrifuged to afford a black precipitate. 6 mL of mixed solvent of tetrahydrofuran and dichloromethane was used to dissolve the precipitate and the mixture was centrifuged at 14000 rpm for 4 min. Finally, the supernatant was subjected to the diffusion of toluene. Rod-like brown crystals were obtained after 3 weeks (yield: 16.6% based on Au, Figure S1).

X-ray crystallographic analysis revealed that **1** crystallized in the *P*-1 space group (Table S1). Each unit cell contains two independent clusters (Figure S2). Cluster **1** consists of 25 Au atoms, 10 $^{i}Pr_2$-bimy ligands, and 7 Br atoms, formulated as $[Au_{25}(^{i}Pr_2\text{-bimy})_{10}Br_7]^{2+}$. The unit cell contains counter anions like NO_3^- and Cl^-, based on which the +2 charge of **1** was determined. The structure of **1** (Figure 1) can be described as two centered Au_{13} icosahedra sharing a vertex, giving rise to a prolate shape with an 1_a:5_b:1_c:5_d:1_e:5_d:1_c:5_b:1_a arrangement of Au atoms (the subscripts designate the positions on the fivefold axis). The four Au_5 pentagons are arranged in a staggered-eclipse-staggered configuration. As such, the cluster conforms to idealized D_{5h} symmetry. The ten N-heterocyclic carbene ligands coordinate to the two outer Au (5_b) pentagons. Of the seven bromides, five are doubly bridging the two inner Au (5_d) pentagons while the remaining two terminally coordinated to the two outermost Au (1_a) atoms. The rod-like metal core measures about 1.1 nm along the fivefold axis (Figure S3). The Au-Au bond lengths, averaged in accord with D_{5h} symmetry, are: Au_a-Au_b, 2.935 Å, Au_b-Au_c, 2.723 Å, Au_c-Au_d, 2.778 Å, Au_b-Au_d, 2.898 Å, Au_d-Au_e, 2.857 Å, Au_a-Au_c, 2.736 Å, Au_c-Au_e, 2.811 Å. It can be seen that intra-icosahedral Au-Au bonds are significantly shorter than those on the surface as well as those between the two icosahedra (Figure S4).

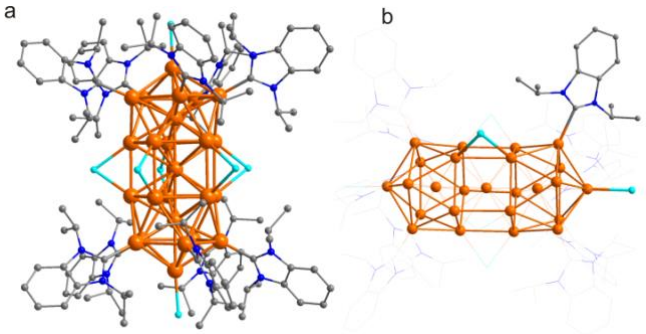

Figure 1. Crystal structure of $[Au_{25}(^{i}Pr_2\text{-bimy})_{10}Br_7]^{2+}$. (a) Overall structure and (b) Au_{25} metal core, showing the binding modes between Au atoms and the ligands (one of each is highlighted). Color legend: orange, Au; cyan, Br; blue, N; gray, C. H atoms are omitted for clarity.

The average Au-Br bond distance of the doubly-bridging bromides is 2.563 Å which somewhat longer than that of 2.442 Å of the terminal bromides. The ten NHC ligands coordinate to the ten Au_b atoms forming Au-C bonds. The average Au-C distance is 2.069 Å, suggesting strong bonding interaction. For comparison, this value is slightly larger than that in $^{i}Pr_2$-bimyAuBr (1.978 Å),[44] but somewhat less than that in $^{i}Pr_2$-bimy self-assembled gold monolayer (2.118 Å).[34] Interestingly, structure of **1** quite resembles that of Au_{25},[45]or Pt_2Ag_{23} protected by tertiary phosphines,[46] indicating that in shaping structure of nanoclusters, NHCs can adopt similar binding modes with tertiary phosphines. The similar observation has also been revealed in organometallic complexes. Cluster **1** is also closely related to the series of vertex-sharing biicosahedral bimetallic (Au-Ag) and trimetallic (Au-Ag-M where M = Ni, Pd, Pt) clusters stabilized by phosphine and halide ligands reported by Teo and coworkers as early as the 1980s.[47-48]

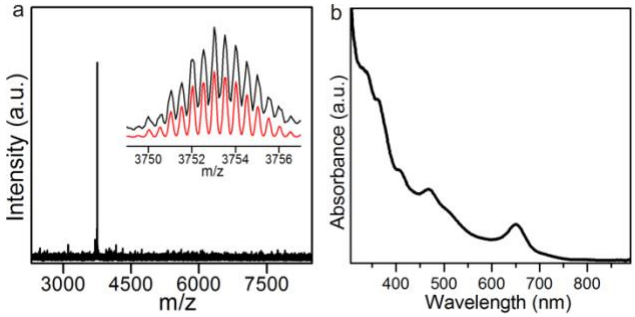

Figure 2. (a) ESI-MS spectrum of **1** crystals dissolved in CH_2Cl_2. Inset: the experimental (black trace) and simulated (red trace) isotopic patterns of $[Au_{25}(^{i}Pr_2\text{-bimy})_{10}Br_7]^{2+}$. (b) UV-Vis spectrum of crystals of **1** dissolved in CH_2Cl_2.

The composition of **1** was confirmed by electrospray ionization mass spectrometry (ESI-MS) under positive ion mode in CH_2Cl_2. As shown in Figure 2a, the ESI-MS spectrum revealed only a single peak at 3756 m/z, corresponding to $[Au_{25}(^{i}Pr_2\text{-bimy})_{10}Br_7]^{2+}$. Perfect agreement was observed between the experimental spectrum and simulated isotopic distribution pattern.

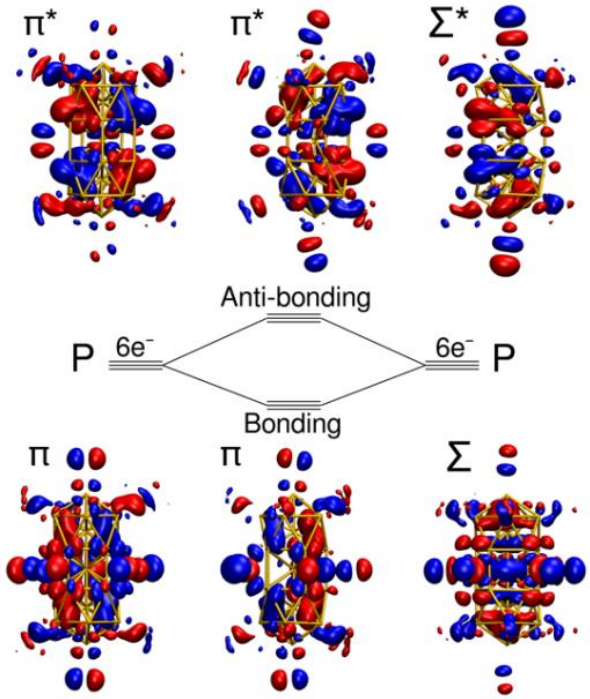

Figure 3. Visualization of the Π and Σ symmetries of the six highest occupied molecular orbitals HOMO-5 to HOMO (with 12 electrons), marked in Figure S5. HOMO-5 to HOMO-3 (bottom) have clear bonding characters with respect to the horizontal place bisecting the Au_{25} metal core, while HOMO-2 to HOMO (top) have antibonding characters. The center graph shows the schematic energy splitting of the bonding/anti-bonding orbitals formed as combination of P-type orbitals in each icosahedral half-core.

Electronic structure and optical properties. DFT calculations were employed to investigate the ground-state electronic structure of **1** (see Experimental section for technical details). The calculated HOMO-LUMO energy gap (Figure S5) is significant, 1.52 eV, which implies a good electronic stability of the cluster. However, the chemical composition of **1** implies 16 metallic free electrons,[49] which is not an expected shell-closing electron number of metal clusters. This prompted us to look further to the reasons of the electronic stability. According to Figure S5a, six highest occupied orbitals of the system have clear P-type symmetries when the symmetry analysis is done in one of the icosahedral half-cores of the cluster. Visualization of the orbitals (Figure 3) reveals that these six orbitals (with overall Π and Σ symmetries) are arranged in two groups having a clear bonding and antibonding characters with respect to the plane bisecting the core. This implies a strong interaction of the superatom P-type orbitals between the icosahedral half-cores, indicating that the free-electron count of 16 of the whole cluster can be understood as a strongly interacting dimer of two 8-electron systems.

1 exhibits a distinct optical absorption spectrum in the UV-Vis region (Figure 2b) with five features: three shoulders at 333, 362, and 406 nm as well as two peaks at 469 and 650 nm. The absorption spectrum of **1** is very similar to that of phosphine and thiolate co-protected $Au_{25}(PPh_3)_{10}(SC_2H_4Ph)_5Cl_2$ (**2**) (Figure 4b), suggesting that discrete electronic states of Au_{25} with similar metal framework are most likely dictated by the vertex-sharing biicoshedral metal architecture.

Time-dependent DFT was employed to compute and analyze the optical absorption spectrum (see Experimental section for technical details). Figure S6 shows the comparison of the calculated and measure spectra. We were able to identify the same five features in the computed spectrum as in the measured data, although the two lowest-energy peaks are somewhat red-shifted in the calculations. Analysis of these five features in terms of transition contribution maps (TCMs) (Figure S7) decomposing the state symmetries in the D_{5h} point group (Figure S5b) shows that the two lowest-energy peaks are mostly single-state transition between symmetries A_2'' to A_1'' (650 nm in the exp. data) and E_1'' to E_1' (469 nm) while the higher-energy transition have multi-state features with contributions from ligands as well.

Excellent stability of 1 in solution. The stability of **1** was investigated by tracking its UV-vis spectrum under thermal treatments. As shown in Figure 4a, the UV-vis profile of **1** was practically unchanged upon heating in 1,2-dichloroethane at 80 °C for 12 h, indicating ultrahigh thermal stability. The intensity of the peak at 650 nm was plotted as a function of heating time in Figure 4d (black curve). The relative intensity showed almost no degradation in the thermal measurement, suggesting that there is no decomposition. Note that **1** is also highly stable in other solvents such as tetrahydrofuran (Figure S8). For comparison, the stability of thiol and phosphine stabilized Au_{25} NCs were also investigated under the same conditions. As shown in Figure 4b, UV-vis spectra of **2**, $Au_{25}(PPh_3)_{10}(SC_2H_4Ph)_5Cl_2$, deteriorates progressively in the 12 h heating period, and the relative absorbance intensity of the peak at 650 nm decreases significantly (Figure 4d, red curve). Furthermore, thiol-protected $Au_{25}(SC_2H_4Ph)_{18}$ (**3**) also exhibits much worse stability than that of **1** (Figure 4c and pink curve in Figure 4d).[50] Earlier DFT calculations on a mixed-ligand $[Au_{11}(PPh_3)_7(NHC^{i\text{-}Pr})Cl_2]Cl$ cluster have shown,[51] that the gold-carbene bond can be stronger than gold-phosphine bond by up to 0.9 eV. This explains also the observed superior thermal stability of **1** over **2** in this work.

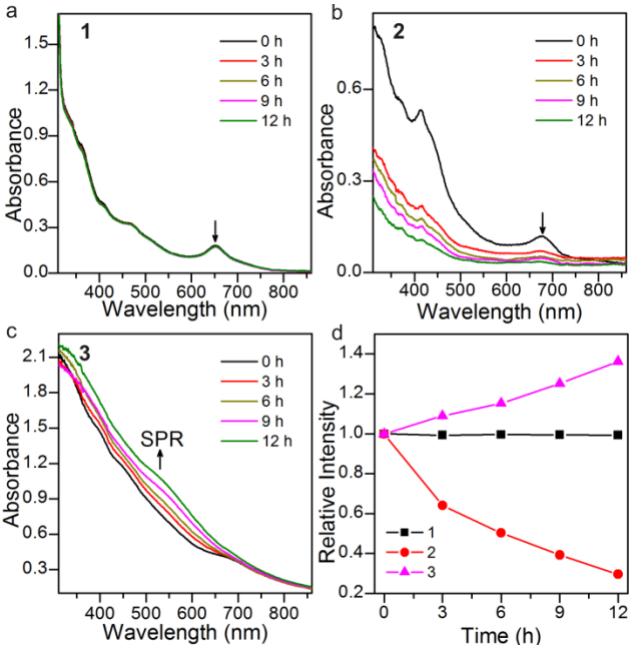

Figure 4. Comparison stabilities of Au_{25} nanoclusters stabilized by different organic ligands. (a). UV-vis spectra of **1** from 0-12 h heating in 1,2-dichloroethane. (b). UV-vis spectra of **2** from 0-12 h heating in 1,2-dichloroethane. (c). UV-vis spectra of **3** from 0-12 h heating in 1,2-dichloroethane. (d). Relative absorbance intensity of peaks marked with arrow (for **1**, 650 nm; for **2**, 675 nm; for **3**, 520 nm).

Surface reactivity and catalytic performance. Next, we explored the functionality of **1** as a homogeneous catalyst. Here we chose the cycloisomerization of alkynyl amines to form indoles as a model reaction. Indoles are important heterocycles which are broadly used in material science and biology. [52] The catalytic reaction was conducted by adding 1.5 % mmol (based on Au) of **1** to a solution of alkynyl amine in organic solvents. As envisioned, 1.5 % mmol catalyst (calculated based on Au atom) succeeded in accelerating the cycloisomerization reaction of N-(2-ethylnylphenyl)-4-methylbenzenesulfonamide to 1-tosyl-1H-indole at 25 °C in 10 h (Table S2, entry 1). The catalytic conditions were optimized by exploring the effects of solvent, time and temperature. The optimal conditions were identified at 50 °C in 1,2-dichloroethane, providing the desired product with over 99% yield. Of note, the reaction generally worked well in aprotic solvents (Table S2, entry 2-5). As illustrated in Figure 5, the cluster displayed an extremely high activity in cycloisomeriza-tion of alkynyl amines at 50 °C as its conversion close to 100% after 10 h. Moreover, the catalyst is stable during the catalytic process, as practically no apparent changes in the UV-vis spectrum were observed before and after the catalytic reaction (Figure S9). Given the optimal reaction conditions (Table S2, entry 6), the catalytic performance of the other two types of Au_{25} (**2** and **3**) were also compared. As shown in Table S3, **1** showed a much higher yield of over 99% in comparison to **2** or **3**, as well as Au(I) carbene precursors. We attribute the observed excellent catalysis of **1** to its sterically open halide sites, which are, on the basis of DFT

local charge analysis, gaining significant negative charge as donated by the carbene ligands through gold (Table S4).

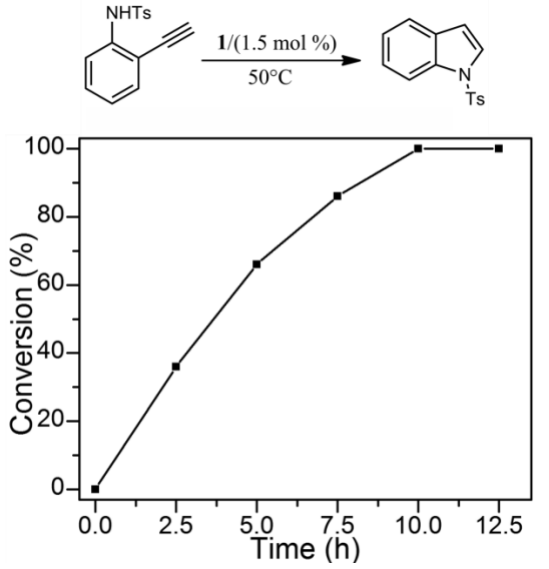

Figure 5. Catalytic performances of 1.5% mmol **1** recorded at different reaction time points for the catalytic cycloisomerization of alkynyl amine.

CONCLUSION

In conclusion, a novel gold nanocluster Au_{25} protected solely by N-heterocyclic carbene ligand was synthesized for the first time via a one-pot reaction protocol. X-ray crystallographic analysis revealed that the cluster consists of two icosahedra sharing a vertex. DFT analysis revealed that the electronic sub-systems of the two icosahedra can be understood as 8-electron configurations that are strongly interacting giving a stable 16-electron system with a large HOMO-LUMO energy gap. The cluster displays ultra high thermal and air stabilities in solution, superior to all other reported Au_{25} nanoclusters. In addition, **1** exhibits high catalytic activity and stability in the cycloisomerization of alkynyl amines to indoles at 50 °C. This work paves ways to use heterocyclic carbene stabilized metal nanoclusters in homogenous catalysis. Finally, it is hoped that, in analogy to its phosphine stabilized kins, [47-48] the biicosahedral framework can be extended to polyicosahedral architecture which, given their superior thermal and air stabilities, may find other applications in nanotechnology that are difficult to fill with other metal cluster systems.

ASSOCIATED CONTENT

The Supporting Information is available free of charge on the ACS Publications website including experimental and computational details and additional data (PDF) and the crystallographic data (CIF).

AUTHOR INFORMATION

Corresponding Author

*nfzheng@xmu.edu.cn

*hannu.j.hakkinen@jyu.fi

Author Contributions

§H. S. and G. D. contributed equally to this work.

ACKNOWLEDGMENT

We thank the National Key R&D Program of China (2017YFA0207302) and the NSF of China (21890752, 21731005, 21420102001, 21721001) for financial support. The computational work in the University of Jyväskylä was supported by the Academy of Finland through HH's Academy Professorship. HH acknowledges support from China's National Innovation and Intelligence Introduction Base visitor program. SK thanks the Väisälä Foundation for a personal PhD study grant. The computations were made at the CSC supercomputing center in Finland.

REFERENCES

(1) Liu, P. X.; Qin, R. X.; Fu, G.; Zheng, N. F. Surface Coordination Chemistry of Metal Nanomaterials. *J. Am. Chem. Soc.* **2017,** *139*, 2122-2131.

(2) Li, G.; Jin, R. Atomically Precise Gold Nanoclusters as New Model Catalysts. *Acc. Chem. Res.* **2013,** *46*, 1749-1758.

(3) Yamazoe, S.; Koyasu, K.; Tsukuda, T. Nonscalable Oxidation Catalysis of Gold Clusters. *Acc. Chem. Res.* **2014,** *47*, 816-824.

(4) Lv, C.; Cheng, H.; He, W.; Shah, M. I. A.; Xu, C.; Meng, X.; Jiao, L.; Wei, S.; Li, J.; Liu, L.; Li, Y. Pd_3 Cluster Catalysis: Compelling Evidence from In Operando Spectroscopic, Kinetic, and Density Functional Theory Studies. *Nano Research* **2016,** *9*, 2544-2550.

(5) Fu, F.; Xiang, J.; Cheng, H.; Cheng, L.; Chong, H.; Wang, S.; Li, P.; Wei, S.; Zhu, M.; Li, Y. A Robust and Efficient Pd3 Cluster Catalyst for the Suzuki Reaction and Its Odd Mechanism. *ACS Catalysis* **2017,** *7*, 1860-1867.

(6) Wang, Y.; Wan, X.-K.; Ren, L.; Su, H.; Li, G.; Malola, S.; Lin, S.; Tang, Z.; Häkkinen, H.; Teo, B. K.; Wang*, Q.-M.; Zheng*, N. Atomically Precise Alkynyl-Protected Metal Nanoclusters as a Model Catalyst: Observation of Promoting Effect of Surface Ligands on Ca-talysis by Metal Nanoparticles *J. Am. Chem. Soc.* **2016,** *138*, 3278-3281.

(7) Yan, J.; Zhang, J.; Chen, X.; Malola, S.; Zhou, B.; Selenius, E.; Zhang, X.; Yuan, P.; Deng, G.; Liu, K.; Su, H.; Teo, B. K.; Häkkinen*, H.; Zheng, L.; Zheng*, N. Thiol-stabilized atomically precise, superatomic silver nanoparticles for catalysing cycloisomerization of alkynyl amines. *Natl. Sci. Rev.* **2018,** *5*, 694-702.

(8) Jin, R.; Zeng, C.; Zhou, M.; Chen, Y. Atomically Precise Colloidal Metal Nanoclusters and Nanoparticles: Fundamentals and Opportunities. *Chem. Rev.* **2016,** *116*, 10346-10413.

(9) Chakraborty, I.; Pradeep, T. Atomically Precise Clusters of Noble Metals: Emerging Link between Atoms and Nanoparticles. *Chem. Rev.* **2017,** *117*, 8208-8271.

(10) Yan, J. Z.; Teo, B. K.; Zheng, N. F. Surface Chemistry of Atomically Precise Coinage-Metal Nanoclusters: From Structural Control to Surface Reactivity and Catalysis. *Acc. Chem. Res.* **2018,** *51*, 3084-3093.

(11) Nasaruddin, R. R.; Chen, T.; Yan, N.; Xie, J. Roles of thiolate ligands in the synthesis, properties and catalytic application of gold nanoclusters. *Coord. Chem. Rev.* **2018,** *368*, 60-79.

(12) Fernando, A.; Weerawardene, K. L. D. M.; Karimova, N. V.; Aikens, C. M. Quantum Mechanical Studies of Large Metal, Metal Oxide, and Metal Chalcogenide Nanoparticles and Clusters. *Chem. Rev.* **2015,** *115*, 6112-6216.

(13) Cook, A. W.; Hayton, T. W. Case Studies in Nanocluster Synthesis and Characterization: Challenges and Opportunities. *Acc. Chem. Res.* **2018,** *51*, 2456-2464.

(14) Hossain, S.; Niihori, Y.; Nair, L. V.; Kumar, B.; Kurashige, W.; Negishi, Y. Alloy Clusters: Precise Synthesis and Mixing Effects. *Acc. Chem. Res.* **2018,** *51*, 3114-3124.

(15) Lei, Z.; Wan, X.-K.; Yuan, S.-F.; Guan, Z.-J.; Wang, Q.-M. Alkynyl Approach toward the Protection of Metal Nanoclusters. *Acc. Chem. Res.* **2018,** *51*, 2465-2474.

(16) Sharma, S.; Chakrahari, K. K.; Saillard, J.-Y.; Liu, C. W. Structurally Precise Dichalcogenolate-Protected Copper and Silver Superatomic Nanoclusters and Their Alloys. *Acc. Chem. Res.* **2018,** *51*, 2475-2483.

(17) Zhang, Q.-F.; Chen, X.; Wang, L.-S. Toward Solution Syntheses of the Tetrahedral Au20 Pyramid and Atomically Precise Gold Nanoclusters with Uncoordinated Sites. *Acc. Chem. Res.* **2018,** *51*, 2159-2168.

(18) Bellon, P.; Manassero, M.; Sansoni, M. Crystal and molecular structure of triiodoheptakis[tris(p-fluorophenyl)phosphine]undecagold. *J. Chem. Soc., Dalton Trans.* **1972,** 1481-1487.
(19) Schmid, G.; Pfeil, R.; Boese, R.; Bandermann, F.; Meyer, S.; Calk, G.; VeldenJ. $Au_{55}[P(C_6H_5)_3]_{12}Cl_6$-ein Goldcluster ungewohnlicher Grofie. *Chem. Ber.* **1981,** *114*, 3634- 3642.
(20) Mingos, D. M. P. Structural and bonding patterns in gold clusters. *Dalton Trans.* **2015,** *44*, 6680-6695.
(21) Jadzinsky, P.; Calero, G.; Ackerson, C.; Bushnell, D.; Kornberg, R. Structure of a Thiol Monolayer–Protected Gold Nanoparticle at 1.1 Å Resolution. *Science* **2007,** *318*, 430-433.
(22) Yang, H. Y.; Wang, Y.; Huang, H. Q.; Gell, L.; Lehtovaara, L.; Malola, S.; Häkkinen, H.; Zheng, N. F. All-Thiol-Stabilized Ag_{44} and $Au_{12}Ag_{32}$ Nanoparticles with Single-Crystal Structures. *Nature Commun.* **2013,** *4*, 2422.
(23) Maity, P.; Wakabayashi, T.; Ichikuni, N.; Tsunoyama, H.; Xie, S.; Yamauchi, M.; Tsukuda, T. Selective synthesis of organogold magic clusters Au54(C≡CPh)26. *Chem. Commun.* **2012,** *48*, 6085-6087.
(24) Wan, X. K.; Tang, Q.; Yuan, S. F.; Jiang, D. E.; Wang, Q. M. Au_{19} nanocluster featuring a V-shaped alkynyl-gold motif. *J. Am. Chem. Soc.* **2015,** *137*, 652-5.
(25) Wang, Y.; Su, H. F.; Xu, C. F.; Li, G.; Gell, L.; Lin, S. C.; Tang, Z. C.; Häkkinen, H.; Zheng, N. F. An Intermetallic $Au_{24}Ag_{20}$ Superatom Nanocluster Stabilized by Labile Ligands. *J. Am. Chem. Soc.* **2015,** *137*, 4324-4327.
(26) Wan, X.-K.; Wang, J.-Q.; Nan, Z.-A.; Wang, Q.-M. Ligand effects in catalysis by atomically precise gold nanoclusters. *Sci. Adv.* **2017,** *3*, e1701823.
(27) Dreier, T. A.; Andrea Wong, O.; Ackerson, C. J. Oxidative decomposition of $Au_{25}(SR)_{18}$ clusters in a catalytic context. *Chem. Commun.* **2015,** *51*, 1240-1243.
(28) Yang, H.; Wang, Y.; Lei, J.; Shi, L.; Wu, X.; Makinen, V.; Lin, S.; Tang, Z.; He, J.; Häkkinen, H.; Zheng, L.; Zheng*, N. Ligand-Stabilized $Au_{13}Cu_x$ (x = 2, 4, 8) Bimetallic Nanoclusters: Ligand Engineering to Control the Exposure of Metal Sites. *J. Am. Chem. Soc.* **2013,** *135*, 9568-9571.
(29) Monfredini, A.; Santacroce, V.; Marchiò, L.; Maggi, R.; Bigi, F.; Maestri, G.; Malacria, M. Semi-Reduction of Internal Alkynes with Prototypical Subnanometric Metal Surfaces: Bridging Homogeneous and Heterogeneous Catalysis with Trinuclear All-Metal Aromatics. *ACS Sustainable Chem. Eng.* **2017,** *5*, 8205-8212.
(30) Zhukhovitskiy, A. V.; MacLeod, M. J.; Johnson, J. A. Carbene Ligands in Surface Chemistry: From Stabilization of Discrete Elemental Allotropes to Modification of Nanoscale and Bulk Substrates. *Chem. Rev.* **2015,** *115*, 11503-32.
(31) Zhukhovitskiy, A. V.; Mavros, M. G.; Van Voorhis, T.; Johnson, J. A. Addressable carbene anchors for gold surfaces. *J. Am. Chem. Soc.* **2013,** *135*, 7418-21.
(32) MacLeod, M. J.; Goodman, A. J.; Ye, H. Z.; Nguyen, H. V.; Van Voorhis, T.; Johnson, J. A. Robust gold nanorods stabilized by bidentate N-heterocyclic-carbene-thiolate ligands. *Nat. Chem.* **2019,** *11*, 57-63.
(33) Wang, G.; Ruhling, A.; Amirjalayer, S.; Knor, M.; Ernst, J. B.; Richter, C.; Gao, H. J.; Timmer, A.; Gao, H. Y.; Doltsinis, N. L.; Glorius, F.; Fuchs, H. Ballbot-type motion of N-heterocyclic carbenes on gold surfaces. *Nat. Chem.* **2017,** *9*, 152-156.
(34) Crudden, C. M.; Horton, J. H.; Ebralidze, II; Zenkina, O. V.; McLean, A. B.; Drevniok, B.; She, Z.; Kraatz, H. B.; Mosey, N. J.; Seki, T.; Keske, E. C.; Leake, J. D.; Rousina-Webb, A.; Wu, G. Ultra stable self-assembled monolayers of N-heterocyclic carbenes on gold. *Nat. Chem.* **2014,** *6*, 409-414.
(35) Crudden, C. M.; Horton, J. H.; Narouz, M. R.; Li, Z.; Smith, C. A.; Munro, K.; Baddeley, C. J.; Larrea, C. R.; Drevniok, B.; Thanabalasingam, B.; McLean, A. B.; Zenkina, O. V.; Ebralidze, II; She, Z.; Kraatz, H. B.; Mosey, N. J.; Saunders, L. N.; Yagi, A. Simple direct formation of self-assembled N-heterocyclic carbene monolayers on gold and their application in biosensing. *Nat. Commun.* **2016,** *7*, 12654.
(36) Bakker, A.; Timmer, A.; Kolodzeiski, E.; Freitag, M.; Gao, H. Y.; Monig, H.; Amirjalayer, S.; Glorius, F.; Fuchs, H. Elucidating the Binding Modes of N-Heterocyclic Carbenes on a Gold Surface. *J. Am. Chem. Soc.* **2018,** *140*, 11889-11892.
(37) Man, R. W. Y.; Li, C. H.; MacLean, M. W. A.; Zenkina, O. V.; Zamora, M. T.; Saunders, L. N.; Rousina-Webb, A.; Nambo, M.; Crudden, C. M. Ultrastable Gold Nanoparticles Modified by Bidentate N-Heterocyclic Carbene Ligands. *J. Am. Chem. Soc.* **2018,** *140*, 1576-1579.
(38) Salorinne, K.; Man, R. W. Y.; Li, C. H.; Taki, M.; Nambo, M.; Crudden, C. M. Water-Soluble N-Heterocyclic Carbene-Protected Gold Nanoparticles: Size-Controlled Synthesis, Stability, and Optical Properties. *Angew. Chem. Int. Ed.* **2017,** *56*, 6198-6202.
(39) Khalili, N. B.; Corrigan, J. F. N-Heterocyclic carbene stabilized Ag-P nanoclusters. *Chem. Commun.* **2015,** *51*, 665-667.
(40) Polgar, A. M.; Weigend, F.; Zhang, A.; Stillman, M. J.; Corrigan, J. F. A N-Heterocyclic Carbene-Stabilized Coinage Metal-Chalcogenide Framework with Tunable Optical Properties. *J. Am. Chem. Soc.* **2017,** *139*, 14045-14048.
(41) Robilotto, T. J.; Bacsa, J.; Gray, T. G.; Sadighi, J. P. Synthesis of a trigold monocation: an isolobal analogue of $[H_3]^+$. *Angew Chem Int Ed Engl* **2012,** *51*, 12077-80.
(42) Tang, Q.; Jiang, D. E. Comprehensive View of the Ligand–Gold Interface from First Principles. *Chem. Mater.* **2017,** *29*, 6908-6915.
(43) Hopkinson, M. N.; Richter, C.; Schedler, M.; Glorius, F. An overview of N-heterocyclic carbenes. *Nature* **2014,** *510*, 485-96.
(44) Huynh, H. V.; Guo, S.; Wu, W. Detailed Structural, Spectroscopic, and Electrochemical Trends of Halido Mono- and Bis(NHC) Complexes of Au(I) and Au(III). *Organometallics* **2013,** *32*, 4591-4600.
(45) Shichibu, Y.; Negishi, Y.; Watanabe, T.; Chaki, N.; Kawaguchi, H.; T., T. Biicosahedral Gold Clusters $[Au_{25}(PPh_3)_{10}(SC_nH_{2n+1})_5Cl_2]^{2+}$ (n=2-18): A Stepping Stone to Cluster-Assembled Materials. *J. Phys. Chem. C* **2007,** *111*, 7845-7847.
(46) Bootharaju, M.; Kozlov, S.; Cao, Z.; Harb, M.; Maity, N.; Shkurenko, A.; Parida, M.; Hedhili, M.; Eddaoudi, M.; Mohammed, O.; Bakr, O.; Cavallo, L.; Basset, J. Doping-Induced Anisotropic Self-Assembly of Silver Icosahedra in $[Pt_2Ag_{23}Cl_7(PPh_3)_{10}]$ Nanoclusters. *J. Am. Chem. Soc.* **2017,** *139*, 1053-1056.
(47) Teo, B. K.; Zhang, H. Polyicosahedricity: icosahedron to icosahedron of icosahedra growth pathway for bimetallic (Au- Ag) and trimetallic (Au-Ag-M; M = Pt, Pd, Ni) supraclusters; synthetic strategies, site preference, and stereochemical principles. *Coord. Chem. Rev.* **1995,** *143*, 611-636.
(48) Teo, B. K.; Zhang, H. Clusters of clusters: Self-organization and self-similarity in the intermediate stages of cluster growth of Au-Ag supraclusters. *Proc. Nat. Acad. Sci.* **1991,** *88*, 5067-5071.
(49) Walter, M.; Akola, J.; Acevedo, O. L.; Jadzinsky, P. D.; Calero, G.; Ackerson, C. J.; Whetten, R. L.; Gronbeck, H.; Häkkinen, H. A unified view of ligand-protected gold clusters as superatom complexes. *Proc. Natl. Acad. Sci.* **2008,** *105*, 9157–9162.
(50) Zhu, M.; Aikens, C.; Hollander, F.; Schatz, G.; Jin, R. Correlating the Crystal Structure of A Thiol-Protected Au_{25} Cluster and Optical Properties. *J. Am. Chem. Soc.* **2008,** *130*, 5883–5885.
(51) Narouz, M. R.; Osten, K. M.; Unsworth, P. J.; Man, R. W. Y.; Salorinne, K.; Takano, S.; Tomihara, R.; Kaappa, S.; Malola, S.; Dinh, C.-T.; Padmos, J. D.; Ayoo, K.; Garrett, P. J.; Nambo, M.; Horton, J. H.; Sargent, E. H.; Häkkinen, H.; Tsukuda, T.; Crudden, C. M. N-heterocyclic carbene-functionalized magic-number gold nanoclusters. *Nat. Chem.* **2019,** *11*, doi:10.1038/s41557-019-0246-5.
(52) Sravanthi, T. V.; Manju, S. L. Indoles - A promising scaffold for drug development. *Eur. J. Pharm. Sci.* **2016,** *91*, 1-10.
(53) Calhorda, M. J.; Ceamanos, C.; Crespo, O.; Gimeno, M. C.; Laguna, A.; Larraz, C.; Vaz, P. D.; Villacampa, M. D. Heteropolynuclear gold complexes with metallophilic interactions: modulation of the luminescent properties. *Inorg. Chem.* **2010,** *49*, 8255-8269.
(54) Asekunowo, P. O.; Haque, R. A.; Razali, M. R.; Budagumpi, S. Benzimidazole-based silver(I)-N-heterocyclic carbene complexes as anti-bacterials: synthesis, crystal structures and nucleic acids interaction studies. *App. Org. Chem.* **2015,** *29*, 126-137.
(55) Collado, A.; Gomez-Suarez, A.; Martin, A. R.; Slawin, A. M.; Nolan, S. P. Straightforward synthesis of [Au(NHC)X] (NHC = N-heterocyclic carbene, X = Cl, Br, I) complexes. *Chem. Commun.* **2013,** *49*, 5541-5543.
(56) Shu, C.; Chen, C.; Chen, W.; Ye, L. Flexible and Practical Synthesis of Anthracenes through Gold-Catalyzed Cyclization of oAlkynyldiarylmethanes. *Org. Lett.* **2013,** *15*, 5542-5545.
(57) Song, Y.; Jin, S.; Kang, X.; Xiang, J.; Deng, H.; Yu, H.; Zhu, M. How a Single Electron Affects the Properties of the "Non-Superatom" Au-25 Nanoclusters. *Chemistry of Materials* **2016,** *28*, 2609-2617.
(58) Sheldrick, G. M. SHELXT - integrated space-group and crystal-structure determination. *Acta Cryst. A* **2015,** *71*, 3-8.
(59) Sheldrick, G. M. A short history of SHELX. *Acta Cryst. A* **2008,** *64*, 112-22.
(60) Dolomanov, O. V.; Bourhis, L. J.; Gildea, R. J.; Howard, J. A. K.; Puschmann, H. OLEX2: a complete structure solution, refinement and analysis program. *J. Appl. Cryst.* **2009,** *42*, 339-341.

(61) Hubschle, C. B.; Sheldrick, G. M.; Dittrich, B. ShelXle: a Qt graphical user interface for SHELXL. *J Appl. Cryst.* **2011,** *44*, 1281-1284.
(62) Enkovaara, J.; Rostgaard, C.; Mortensen, J. J.; Chen, J.; Dulak, M.; Ferrighi, L.; Gavnholt, J.; Glinsvad, C.; Haikola, V.; Hansen, H. A.; Kristoffersen, H. H.; Kuisma, M.; Larsen, A. H.; Lehtovaara, L.; Ljungberg, M.; Lopez-Acevedo, O.; Moses, P. G.; Ojanen, J.; Olsen, T.; Petzold, V.; Romero, N. A.; Stausholm-Moller, J.; Strange, M.; Tritsaris, G. A.; Vanin, M.; Walter, M.; Hammer, B.; Hakkinen, H.; Madsen, G. K.; Nieminen, R. M.; Norskov, J. K.; Puska, M.; Rantala, T. T.; Schiotz, J.; Thygesen, K. S.; Jacobsen, K. W. Electronic structure calculations with GPAW: a real-space implementation of the projector augmented-wave method. *J. Phys. Condens. Matter.* **2010,** *22*, 253202.
(63) Perdew, J.; Burke, K.; Ernzerhof, M. Generalized Gradient Approximation Made Simple. *Phys. Rev. Lett.* **1996,** *77*, 3865-3868.
(64) Tang, W.; Sanville, E.; Henkelman, G. A grid-based Bader analysis algorithm without lattice bias. *J. Phys. Condens. Matter.* **2009,** *21*, 084204.
(65) Walter, M.; Hakkinen, H.; Lehtovaara, L.; Puska, M.; Enkovaara, J.; Rostgaard, C.; Mortensen, J. J. Time-dependent density-functional theory in the projector augmented-wave method. *J. Chem. Phys.* **2008,** *128*, 244101-2441010.
(66) Sami Malola, L. L., Jussi Enkovaara, Hannu Häkkinen Birth of the Localized Surface Plasmon Resonance in Monolayer-Protected Gold Nanoclusters. *ACS Nano* **2013,** *7*, 10263-10270.
(67) Kaappa, S.; Malola, S.; Hakkinen, H. Point Group Symmetry Analysis of the Electronic Structure of Bare and Protected Metal Nanocrystals. *J. Phys. Chem. A* **2018,** *122*, 8576-8584.

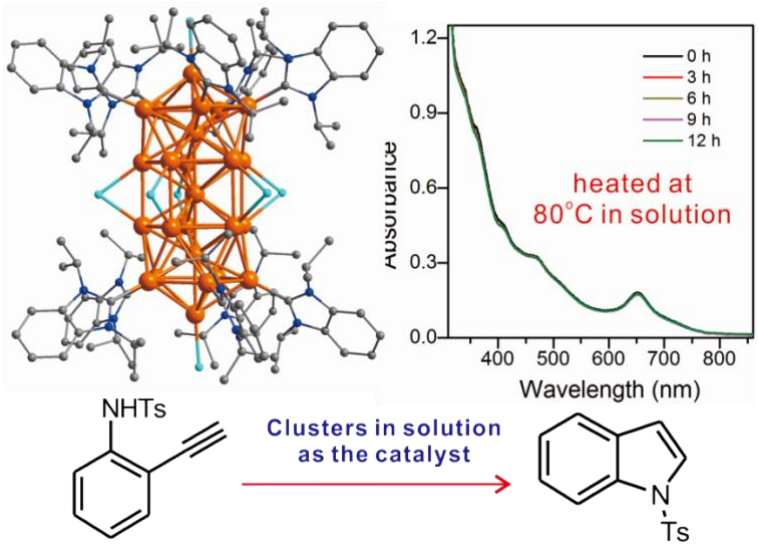
1.2
0.9
0.6
0.3
0.0
Absorbance
400
500
600
700
800
Wavelength (nm)
0 h
3 h
6 h
9 h
12 h
heated at
80°C in solution
NHTs
Clusters in solution
as the catalyst
N
Ts